Available online at http://ijcpe.uobaghdad.edu.iq and www.iasj.net
Iraqi Journal of Chemical and Petroleum Engineering
Vol. 24 No. 4 (December 2023) 47 – 57
EISSN: 2618-0707, PISSN: 1997-4884

Estimation of the Petrophysical Properties of the Lower Cretaceous Yamama (YC) Formation in Siba Field

Zainab A. Hadi [a], Omar F. Al-Fatlawi [a, b], Ali Kadkhodaie [c, *]

a Department of Petroleum Engineering, College of Engineering, University of Baghdad, Baghdad, Iraq
b WASM: Minerals, Energy and Chemical Engineering, Curtin University, WA, Australia
c Earth Sciences Department, Faculty of Natural Sciences, University of Tabriz, Iran

Abstract

In southern Iraq, the Yamama Formation has been a primary carbonate resource since the Lower Cretaceous era. This study covers Siba Field, which is located in southeastern Iraq. This paper will be devoted to a YC unit of study. The most crucial step in reservoir management is petrophysical characterization. The primary goal of this research is to assess the reservoir features and lithology of the Yamama (YC) Formation in the Siba region. Accessible excellent logs include sonic, density, neutron, gamma-ray, SP, and resistivity readings. The Interactive Petrophysics (IP4.4) program examined and estimated petrophysical features such as clay volume, porosity, and water saturation. The optimum approach was the neutron density and clay volume calculation using the Gamma Ray Method (VclGR), it was 0.246 in SB-6 since they are not impacted by anything. The Archie method was chosen due to its suitability for limestone. The lithology and mineralogy of the formations were determined using M-N cross plots; the diagram revealed that the Formation was composed of limestone. The Archie parameter was determined using the Pickett plot and formation water resistivity from the Pickett plot and SP log where the results were similar in all wells (R_W=0.016, m=2.08, n=2.3, a=1.1). In addition, the higher section of the formation has good reservoir qualities such as density is (2.368g/cc), porosity is (PHIE=0.117) in SB-6.

Keywords: petrophysical properties, Yamama formation, Reservoir characterization, Siba field.

Received on 12/11/2022, Received in Revised Form on 30/11/2022, Accepted on 01/12/2022, Published on 30/12/2023

https://doi.org/10.31699/IJCPE.2023.4.5

1- Introduction

In particular, identifying the hydrocarbon- and non-hydrocarbon-bearing zones requires petrophysical analysis, which is crucial for reservoir characterization [1-6]. The petrophysics of any field encompasses the reservoir fluid parameters and reservoir rock qualities that can influence recovery and production levels [7-9]. These characteristics may include porosity, permeability, fluid saturation, and mobility, among other factors. Successful assessments of these qualities aid in forecasting the behavior of complicated reservoir conditions and are required for estimating the hydrocarbon potential of a reservoir system's performance [10-12]. The high degree of form irregularity means that the carbonate components that make up limestone reservoirs hardly ever fit together precisely [13]. Fluids occupy the pore volume or porosity formed throughout the grain beds, also known as the void space. Porosity is caused by different geological, physical, and chemical processes, and it varies a lot between different types of rocks [14-16]. Reservoir characterization is the process of calculating the petrophysical characteristics of the earth's crust using data from seismic, seismic core, and well-log analysis [13, 17, 18]. Reservoir characterization aims to determine the petrophysical characteristics of a reservoir, such as its permeability, and porosity, at any depth and at any location [19, 20]. The non-linearity and variability of the subsurface make reservoir characterization a challenging task [21, 22]. Aside from the lack of a clear mapping between seismic data and well logs, even if one existed, it may not be very general outside of the research region [23]. Identifying the quantity of clay in shale sand is the most crucial step [24]. It is feasible to compute adequate water saturation and effective porosity more precisely if reservoir clay content is known [25]. Reservoir rocks should be capable of transmitting hydrocarbon fluids through their pores [26]. Saturation is the proportion or percentage of pore volume filled by a particular fluid (oil, gas, or water). All saturation figures are based on pore

*Corresponding Author: Name: Ali Kadkhodaie, Email: kadkhodaie_ali@tabrizu.ac.ir

volume rather than reservoir total volume. When appraising a formation, its petrophysical qualities are taken into account. It must be determined precisely [25]. A fluid's saturation level can be expressed as a fraction or a percentage of the total pore volume it occupies (oil, gas, or water). Not the overall volume of the reservoir, but the pore volume is used to calculate all the saturation figures. Formation evaluation analyzes a mixture of measures acquired inside the wellbore to analyze wells for prospective hydrocarbon-bearing rocks [27, 28]. These measurements may include core samples, laboratory fluid property measurements, and well logs. Well logs are regarded as one of the most critical data sources for the geology and petrophysical characteristics of reservoir formations; well logging is essential for determining the production potential of a hydrocarbon reservoir [29-31]. The primary objectives of this study are to identify the lithological layers and shale types in the reservoir using well log data. The logs are interpreted using IP4.4 software to compute the petrophysical properties of clay volume, porosity, and water saturation. Accurate determination of petrophysical properties is crucial in the formation evaluation process. Consequently, precise identification of these properties is of utmost importance.

- The study region

Primarily, the southwestern portion of the project is a sabkha. This field lies adjacent to Siba city, seen in Fig. 1, and is situated within the Basra country's official limits, about 30 kilometers from the eastern portion of the province. The Shatt al-Arab, which acts as the political boundary between Iraq and Iran, flanks the city to the northeast and north. In contrast, the northern and northeastern portions, and the region near the Shatt al-Arab [32-35]. The Siba field's geology is a NE-SW trending anticline with a low relief structure that exhibits a little dip and a moderate fracture system. Between 3800 and 4500 meters under the TVDSS is where the majority of the exploration and development work will be done.

2- Methodology

To investigate petrophysical parameters, this research employed information from well-open hole logs (spontaneous potential, gamma ray, density, sonic, neutron, and resistivity logs). To illustrate the petrophysical properties of the Siba field in the Yamama (YC) Formation, IP4.4 software was used to perform environment modifications, interpret well logs, and display data. The lithology of the reservoir was identified by analyzing gamma-ray, acoustic, and density data using the IP4.4 program. As shown in Fig. 2, the most important steps that we took in this study.

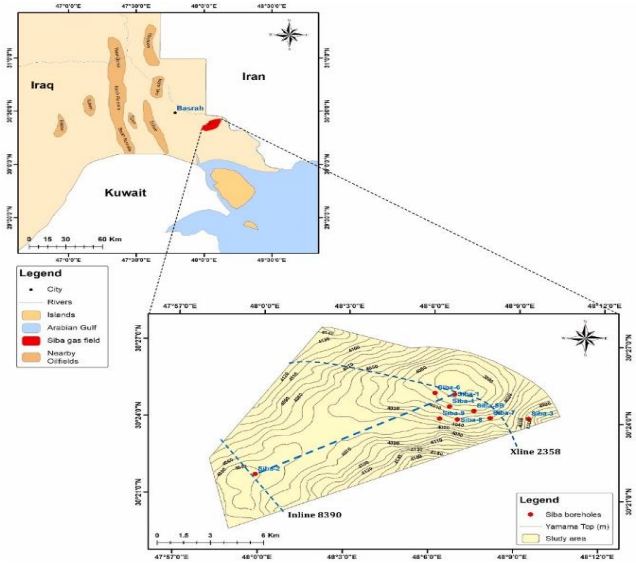

Fig. 1. Detailed Map of the Examined Area [36]

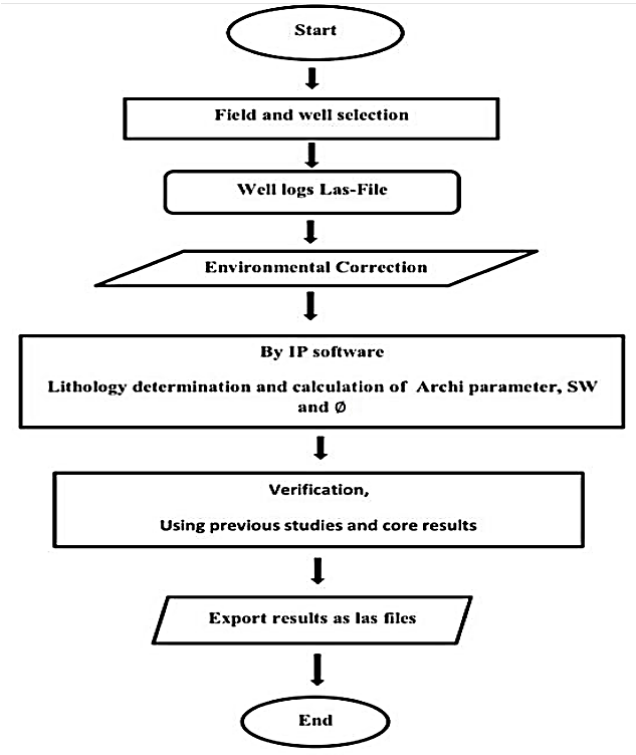

Fig. 2. Flowchart of Well Log Interpretation Approach

3- Results and Discussion

3.1. Environmental Correction

Before commencing the open hole well log analysis, the gamma-ray, neutron, density, and resistivity logs were corrected according to Schlumberger's well log analysis's fundamental Corrections. These adjustments accounted for the shale influence, borehole circumstances, and invasion depth. As previously stated, the raw well logs were rectified before interpretation using Schlumberger's environmental corrections. Fig. 3 shows how the well logs are affected by borehole conditions and how to adjust for them.

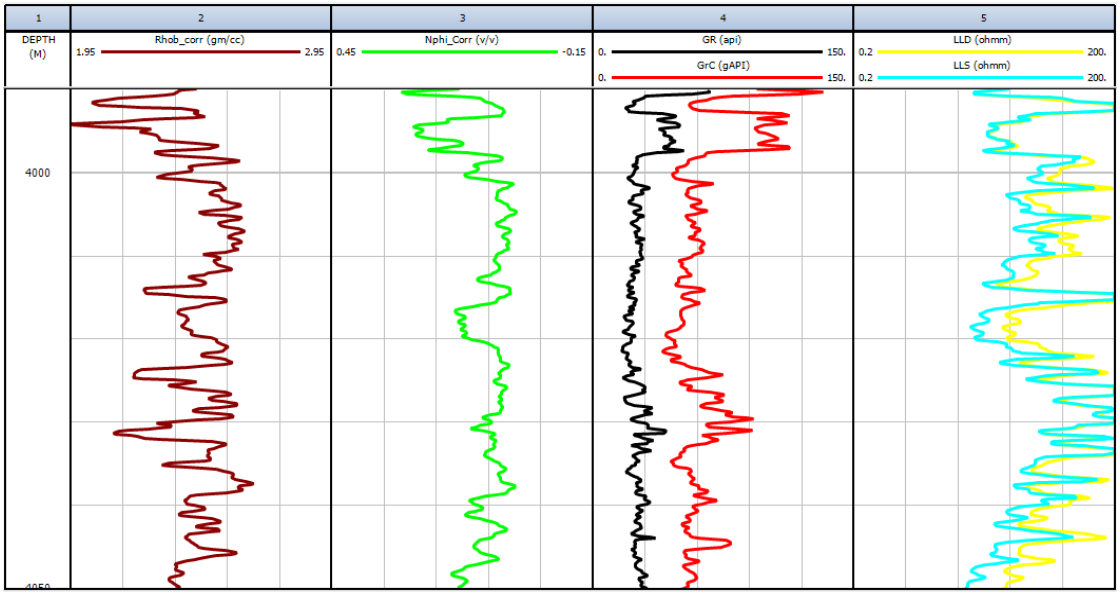

Fig. 3. Correction of the Environment for Logs of SB-6

3.2. Resistivity Formation

Connate water, often known as "formation water," is not contaminated by drilling mud.

a. SP method for Water Resistivity Formation

This method, based on the correlation between Rw and SSP as given in Table 3 is one of the most effective and often used approaches to extrapolate information from the SP log.

To maintain an electrical connection between the SP log and the formation, it is best to record the SP curve in a clean, non-shaly formation with salty base mud, which will result in high Rw values.

b. Water Resistivity Formation according to Pickett Plot

The Pickett cross plot is one of the most basic and successful cross plot approaches. This approach not only calculates water saturation but may also assist in determining: water resistance during creation: formation water resistivity [37].

The Pickett plot was used to provide the value of Rw as shown in Fig. 4 for SB-6.

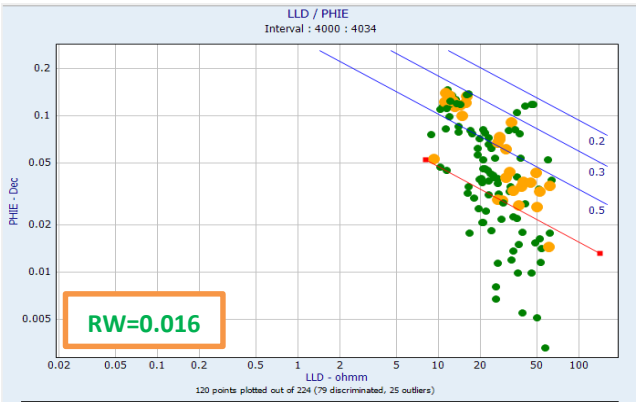

Fig. 4. Rw from Pickett Plot Log in SB-6

Table 1 depicts the resistivity of formation water measured using the SP log and Pickett plot methods in the Yamama (YC) formation in the Siba field.

Table 1. Rw Values Calculated by Two Methods

Wells	The creation of water's resistance	
	RwSP	Rw Pickett plot
SB-2	-	0.0163
SB-3	-	0.0163
SB-4	-	0.016
SB-6	0.0159	0.016

3.3. Clay Volume Calculation

Clay volume is crucial for determining effective porosity and permeability from logs because it changes reservoir heterogeneity. Additionally, the presence of clay in certain types of shale affects the computation of water saturation [38, 39]. Two kinds of indicators are used to estimate clay volume; these approaches must be utilized to assess clay volume, and the wellbore condition must be considered when choosing one [40].

The gamma ray clay calculation, the SP log clay volume, the deep resistivity log clay volume, and the neutron log clay volume are all techniques for determining clay content. Fig. 5 shows the volume of clay computed with a single indication.

The gamma-ray approach is undoubtedly one of the most exact ways to determine clay volume. The accuracy of gamma-ray measurements of clay volume may be affected by various factors, including drilling mud and its effect on the gamma-ray recording. Errors in borehole recording will be reduced by removing the factors that lead to them. The environmental correction may be used to adjust borehole measurements. Drilling mud produces hydrostatic pressure, which is adjusted in the log data. With rising water saturation, actual resistivity increases, leading to overestimating clay volume.

Fig. 5 depicts the clay volume estimation with a single signal of SB-6. Individual indicator formulae are mentioned in Table 3.

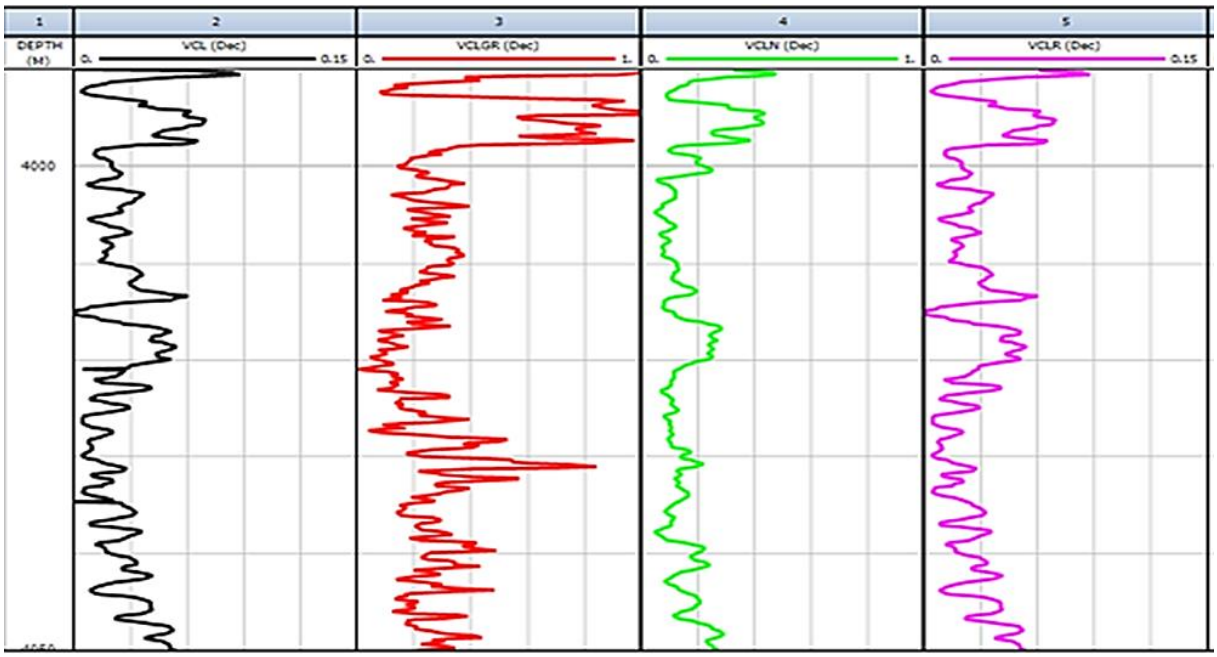

Fig. 5. Volume Calculation of Clay using a Single Indication in SB-6

There are three double clay indications: clay volume derived from neutron and density logs, clay volume derived from neutron and sonic logs, and clay volume derived from density and sonic logs. The neutron and density logs may be affected by borehole conditions and the presence of gas, which may alter the amount of clay that can be measured using the neutron-density approach. Consequently, the clay volume is either inadequate or excessive. This is because these logs are of the pad kind, which causes caving or extreme swelling that impairs their legibility. Since the neutron log measures the amount of formation hydrogen, and gas has a minimal amount of formation hydrogen, gas will cause the neutron porosity readings to be shallow, which could be a reasonable estimate or too low. In certain shale formations, the reliable estimation of clay volume is achievable through density and acoustic logs, as the presence of distributed clay can impact sonic wave measurements. The difference in porosity between neutron and sonic logs is used to estimate the amount of clay. Since clays have a considerable influence on neutron and acoustic porosities, it may be necessary to adjust estimations of clay volume. Fig. 6 shows the volume of clay computed with double indications in SB-6.

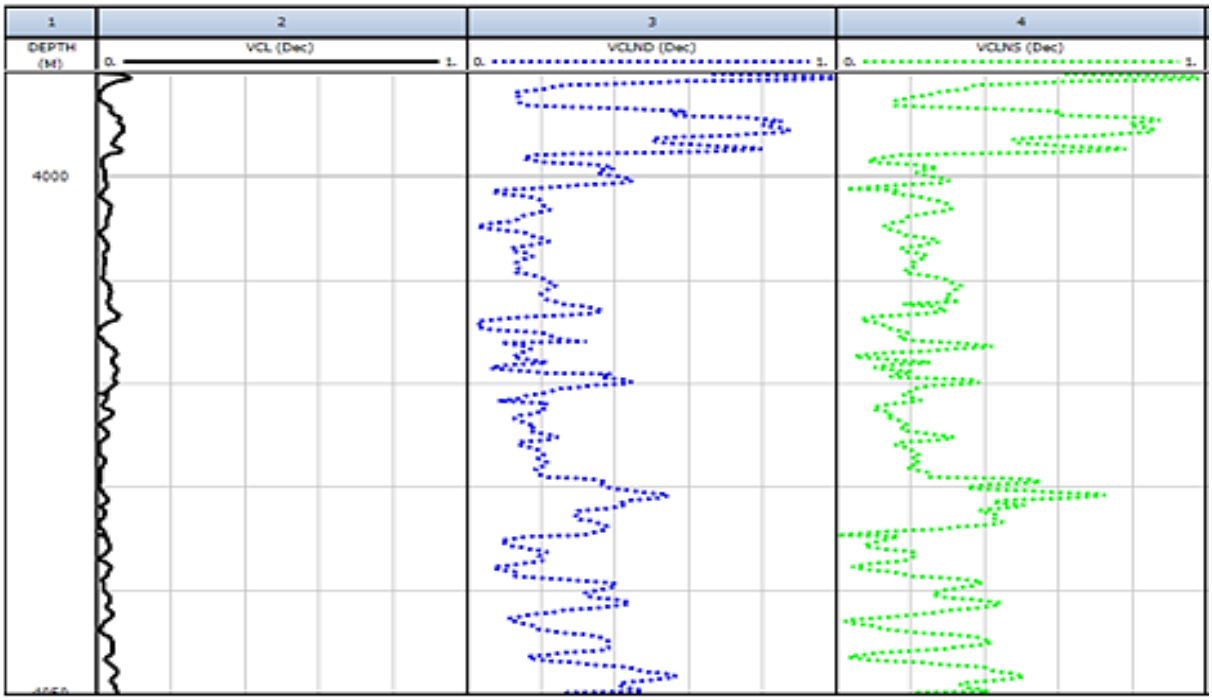

Fig. 6. Clay Volume Estimate with Double Indications in SB-6

3.4. Porosity Estimation

Because porosity affects how much oil a reservoir can store, measuring porosity is crucial for petroleum engineers. The porosity of a rock can be found by comparing the pore volume to the bulk volume. All available techniques for determining effective porosity are applied to compare them to the core's porosity and choose the best condition. The porosity can be calculated by the methods listed in Table 3.

Fig. 7 and Fig. 8 represent the porosity of logs in SB-2. Sonic porosity is the best method for calculating porosity.

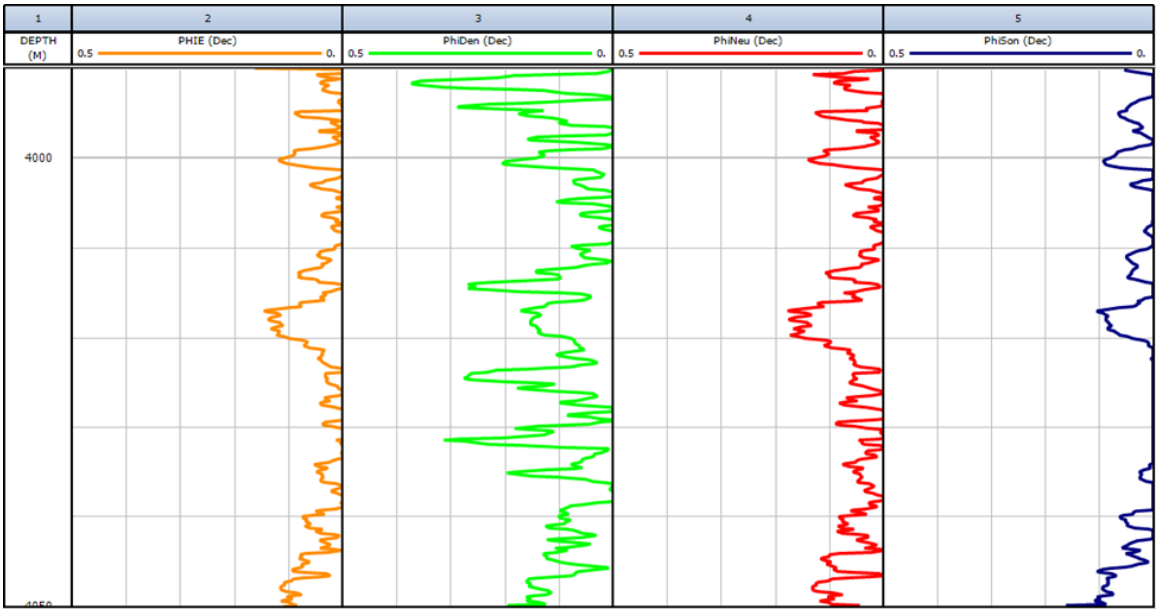

Fig. 7. Effective Porosity by Single Logs in SB-6

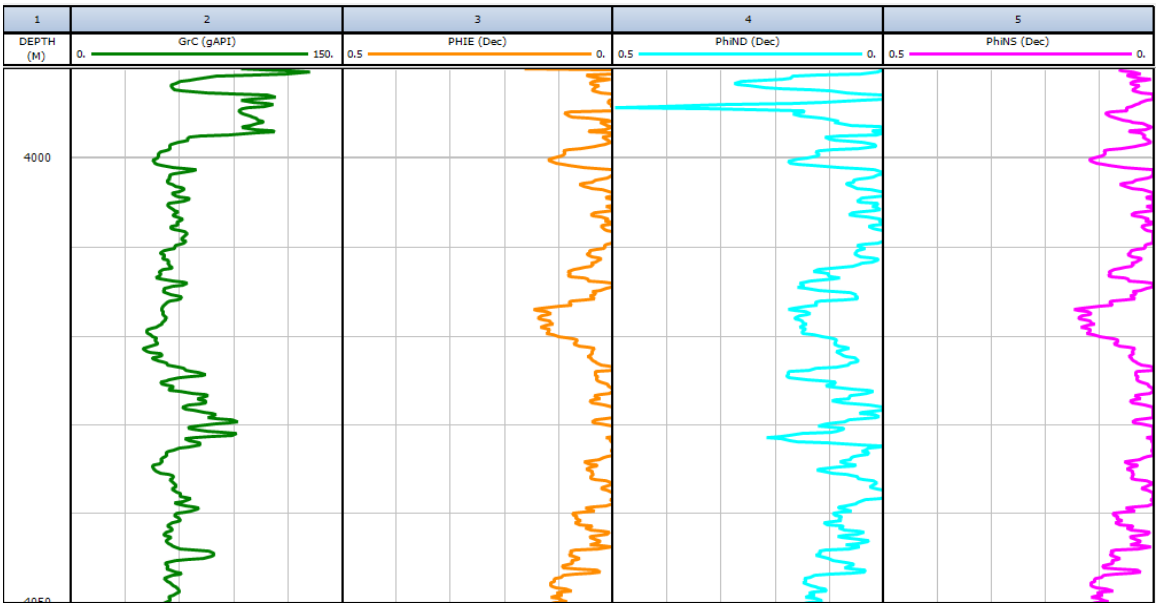

Fig. 8. Effective Porosity by Double Logs in SB-2

3.5. Archie's Parameters Determination

Determining the water saturation level in a reservoir composed of shale and sand is getting increasingly complex. These features are employed in all methods for determining water saturation.

a. Cementation Factor (m)

As the cementation exponent m rises, the pore size distribution flattens out and the number of dead-end channels decreases. It has found widespread use in porous-media engineering studies, as well as hydrocarbon and groundwater exploration [41, 42]. All values are summarized in Table 2.

b. Saturation Exponent (n)

Saturation exponent n is the exponent value in water saturation that connects rock water saturation to the ratio of fluid-filled rock resistivity to true rock resistivity in

Archie's water saturation equation [43, 44]. Table 2 shows the values of all wells.

c. Tortuosity Factor (a)

In porous media, tortuosity is the ratio of the length of a flow route in the primary direction of flow to the length of the medium itself [44]. The tortuosity factor can be determined at the water zone by using equation in Table 3, where Rt=Ro. The values are summarized in Table 2. Fig. 9 of SB-6 depicts the use of the Pickett plot to calculate the values of Archie's parameters.

Table 2. Archie's Parameters Values

Wells	Archie's parameters		
	A	m	n
SB-2	1.1	2.78	2.5
SB-3	1	2	2
SB-4	1.1	2.1	2
SB-6	1.1	2.08	2.3

3.6. M-N Cross Plot

The M-N plot facilitates lithology interpretation in increasingly complicated mineral mixes. These graphs, which incorporate data from the three porosity logs, illustrate the lithology-dependent values M and N. On the sonic density and neutron density cross-plots, M and N are just the slopes of the individual lithology lines. Consequently, M and N are essentially independent of porosity, and a cross plot enables the determination of lithology [37].

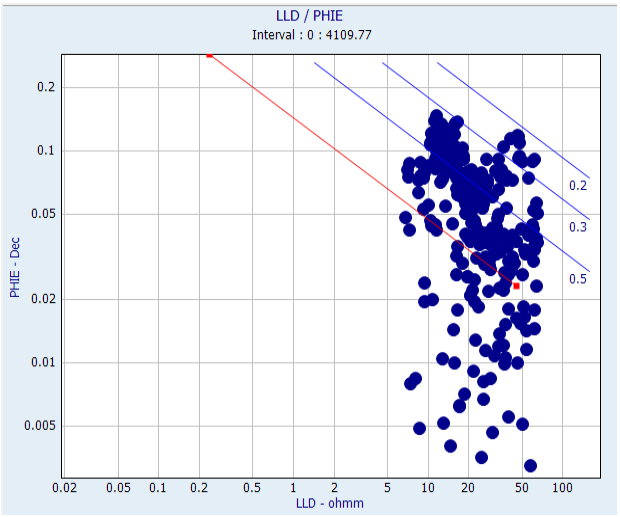

Fig. 9. The Pickett Plot of SB-6

The M-N cross plot for the reservoir unit of the Yamama (YC) formation is illustrated in Fig. 10. It has been found that the Yamama (YC) formation is mainly composed of limestone (representing the calcite area). Moreover, secondary porosity has a distinct orientation.

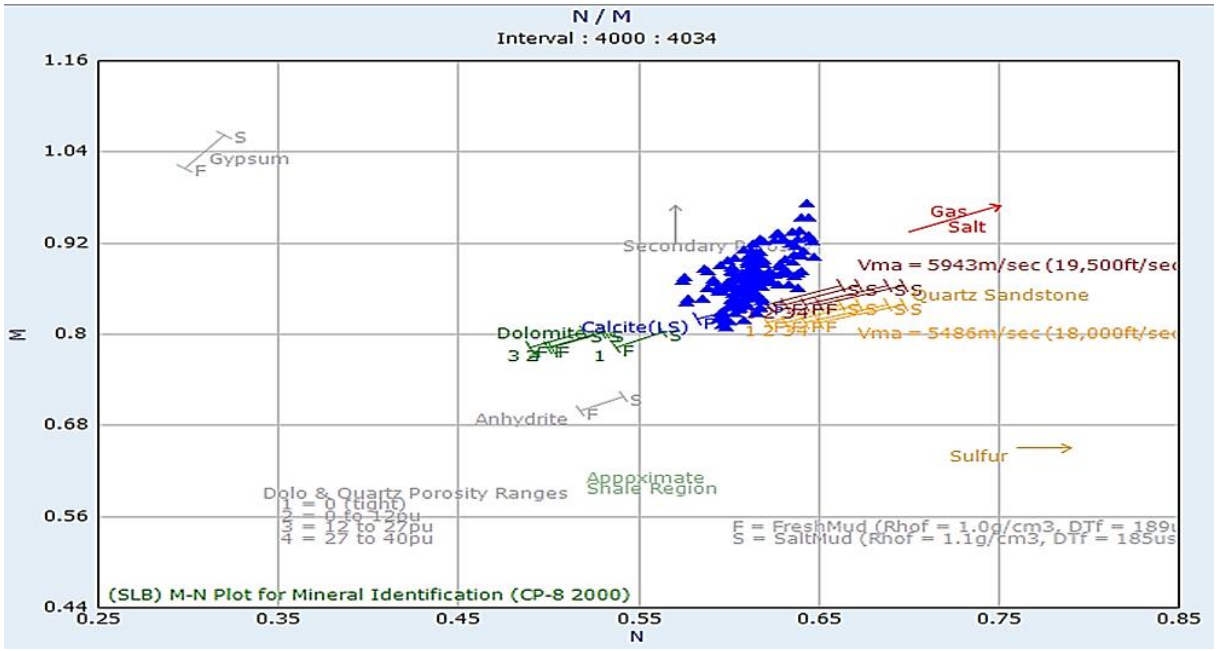

Fig. 10. The M-N Cross Plot for SB-6

3.7. Lithology Determination

The idea underlying lithology identification is the distinctive effects of various minerals on porosity logs. Any combination of the density, neutron, and sonic porosities logs can provide a suitable indicator of the formation lithology [45]. When the matrix's lithology or the ratios of two or more minerals are unknown, it is difficult to predict the porosity. A cross-plot approach is a simple way to show these concepts. A linear cross-plot of density and acoustic porosities is used to establish the matrix lithology when the points (such as limestone, dolomite, or sandstone)2 lie on a curve. It combines the three porous logs.

According to Fig. 11, the Yamama (YC) formation in SB-6 is composed of a limestone unit.

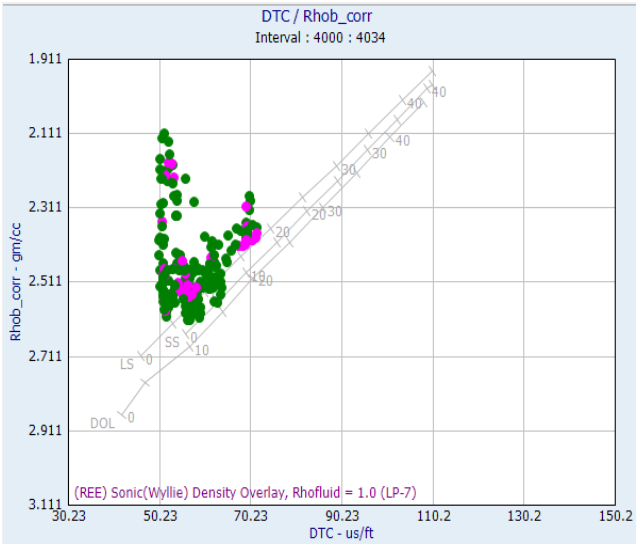

Fig. 11. Limestones at Yamama (YC) Formation in SB-6

3.8 Water Saturation Calculation

Water saturation is the percentage of a specific pore space filled with water. The Archie equation, Dual water model, Indonesia model, Waxman-Smith model, Simandoux model, and modified Simandoux model may all be utilized for measuring the water saturation in the Yamama formation. The Archie model is the most common, although only some combinations are correct. The saturation in shaly sand is overestimated when the Archie model is employed to evaluate water saturation. To choose the best model, all water saturation models in the water zone are compared to the Archie model. These techniques are valid since the water zone was not overstated. So, the right model is chosen when the measured water saturation in the water zone matches Archie's water saturation. In order to evaluate water saturation, the Archie model is utilized. Consideration is given to one of the essential criteria for calculating oil initial in place. In formation evaluation (petro-physical), different saturation models can be used to estimate the amount of water in the rock, depending on whether the reservoir is dirty or clean. The Archie equation, developed in 1942, was the first empirical model for determining water saturation in a pure, simple, uniform pore system[46]. Fig. 12 shows the water saturation calculation of SB-6.

Table 3. Equations Used

Method	Equation
SP method for Water Resistivity Formation	$SP = -(60 + 0.133\,T) * \log\left[\frac{R_{mf}}{R_w}\right]$
Gamma Ray Method	$\mathrm{Vcl} = \frac{GRlog - GRmin}{\mathrm{GRmax} - \mathrm{GRmin}}$
Neutron Method	$\mathrm{Vcl} = \frac{\emptyset_{\mathrm{N}}\ (\mathrm{Shaly\ Sand})}{\emptyset_{\mathrm{N}}\ (\mathrm{Shale\ Zone})}$
Resistivity Method	$Vcl = (\frac{R_{cl}}{Rt})^{\frac{1}{1.5}}$
Sonic Method	$V_{cl} = \frac{\emptyset_{s}\ (\mathrm{Shaly\ Sand})}{\emptyset_{s}\ (\mathrm{shale\ zone})}$
Neutron-Density Method	$V_{cl} = \frac{\emptyset_{\mathrm{N}}\ (\mathrm{Shaly\ Sand}) - \emptyset_{D}\ (\mathrm{Shaly\ Sand})}{\emptyset_{\mathrm{N}}\ (\mathrm{shale\ zone}) - \emptyset_{\mathrm{D}}\ (\mathrm{shale\ zone})}$
Sonic-Density Method	$V_{cl} = \frac{\emptyset_{\mathrm{S}}\ (\mathrm{Shaly\ Sand}) - \emptyset_{D}\ (\mathrm{Shaly\ Sand})}{\emptyset_{\mathrm{S}}\ (\mathrm{shale\ zone}) - \emptyset_{\mathrm{D}}\ (\mathrm{shale\ zone})}$
Neutron-Sonic Method	$V_{cl} = \frac{\emptyset_{\mathrm{N}}\ (\mathrm{Shaly\ Sand}) - \emptyset_{s}\ (Shaly\ \mathrm{Sand})}{\emptyset_{\mathrm{N}}\ (\mathrm{shale\ zone}) - \emptyset_{\mathrm{S}}\ (\mathrm{shale\ zone})}$
Porosity by sonic log	$\emptyset_{\mathrm{sonic}} = \frac{\Delta t_{\mathrm{log}} - \Delta t_{\mathrm{matrix}}}{\Delta t_{\mathrm{fluid}} - \Delta t_{\mathrm{matrix}}}$
Porosity by density log	$\emptyset_{\mathrm{density}} = \frac{\rho_{\mathrm{matrix}} - \rho_{\mathrm{bulk}}}{\rho_{\mathrm{matrix}} - \rho_{\mathrm{fluid}}}$
Porosity by Neutron-Density logs	$\emptyset_{\mathrm{ND}} = \frac{\emptyset_{\mathrm{N}} + \emptyset_{\mathrm{D}}}{2}$
Porosity by Neutron-Sonic logs	$\emptyset_{\mathrm{NS}} = \frac{\emptyset_{\mathrm{N}} + \emptyset_{\mathrm{s}}}{2}$
Tortuosity Factor (a)	$R_o = \frac{a}{\emptyset^m} * R_w$

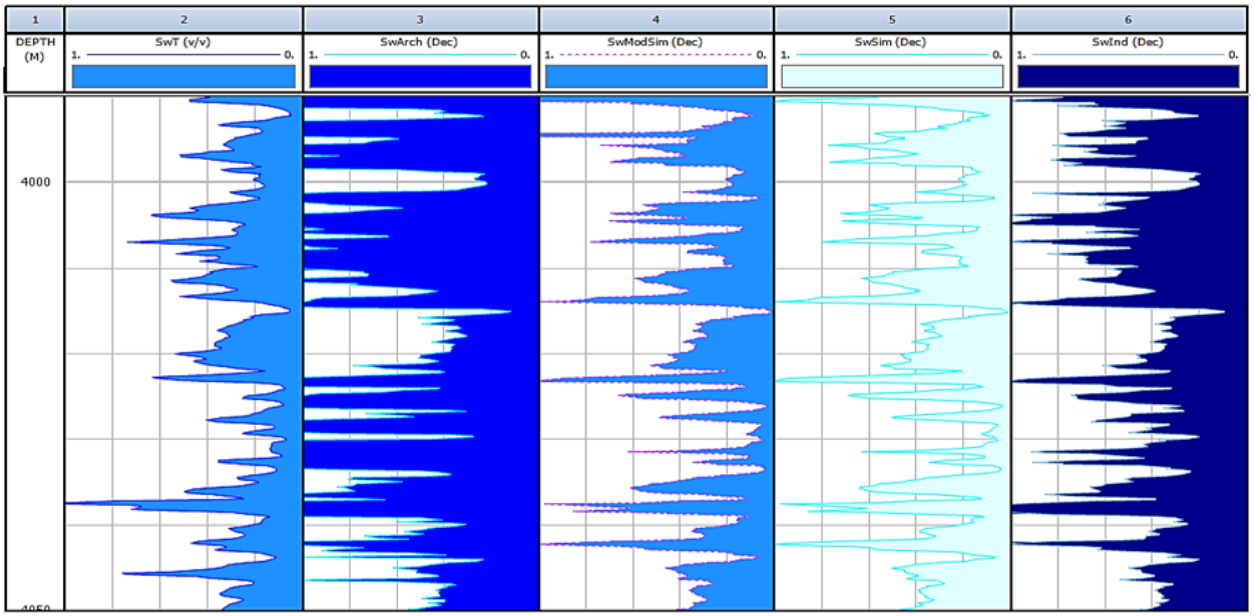

Fig. 12. Water Saturation in SB-6

4- Conclusions

Studying the petrophysical properties of the YC unit in the Siba field produced the following results:

1- The lithology of the Yamama formation (YC unit) was determined as limestone using different cross-plots.
2- The porosity was determined in different ways, but the optimal approach was the neutron density and clay volume calculation using the Gamma Ray Method (VclGR) which yielded a porosity value of 0.117. This method was chosen because it is not impacted by other factors.
3- The Archie parameter was determined using the Pickett plot and formation water resistivity from the Pickett plot and SP log (R_W=0.016, m=2.08, n=2.3, a=1.1) in SB-6. The rest of the results of the wells are shown in Table 2.
4- In order to calculate water saturation (S_W), more than one method was used. However, the Archie method was chosen due to its suitability for limestone. It was (Sw at depth 4000m in SB-6=0.218Dec).

Nomenclature

SP: spontaneous log recording at clean zone, (MV).
R_{mf}: Resistivity of mud filtrate, (ohm-m).
R_w : Resistivity of formation water, (ohm-m).
Vcl stands for the gamma-ray index.
GRlog stands for gamma-ray reading in the zone of interest.
GRmin stands for minimal gamma-ray reading (clean zone) .
GRmax stands for maximum gamma-ray reading (Shale zone).
$ø_n$ (Shaly Sand) stands for Shaly sand zone neutron porosity
$ø_n$ (Shale) stands for shale zone neutron porosity
R_{cl} stands for clay resistivity (Adjacent Shale Bed)
R_t stands for shaly sand resistivity
R_{lim} stands for the resistivity of a hydrocarbon zone that is clean.
$ø_s$ (Shaly Sand) stands for Shaly sand zone sonic porosity
$ø_s$ (Shale)stands for Shale zone sonic porosity
$ø_N$ (Shaly Sand) stands for neutron porosity in Shaly Sand.
$ø_D$ (Shaly Sand) stands for density and porosity at the shaly sand zone.
$ø_N$ (Shale) stands for shale zone neutron porosity.
$ø_D$ (Shale) stands for porosity density in the shale zone.
Δt_{log} stands for time recorded for travel, (µsec/ft)
Δt_{matrix} stands for Matrix travel time, (µsec/ft)
Δt_{fluid} stands for Fluid travel time, (µsec/ft)
$Ø_{density}$ stands for porosity by log of density
ρ_{matrix} stands for Matrix density, gr/cc
ρ_{bulk} stands for the measured mass density, gr/cc
ρ_{fluid} stands for Fluid density, gr/cc
$Ø_{ND}$ stands for neutron density porosity logs
$Ø_{Ns}$ stands for porosity by neutron –sonic logs.
a: tortuosity factor
n: Saturation factor.
M: Cementation factor.
Sw: Water saturation;
Rw: Water Resistivity ohm-m.
Φe: Effective porosity.

References

[1] M. B. Valentín *et al.*, "A deep residual convolutional neural network for automatic lithological facies identification in Brazilian pre-salt oilfield wellbore image logs," *Journal of Petroleum Science and Engineering*, vol. 179, pp. 474-503, 2019, https://doi.org/10.1016/j.petrol.2019.04.030

[2] P. Anumah, S. Mohammed, J. Sarkodie-Kyeremeh, W. N. Aggrey, and A. Morgan, "Petrophysical evaluation of the reservoir in the k - Field, offshore Ghana," in *Society of Petroleum Engineers - SPE Nigeria Annual International Conference and Exhibition 2019, NAIC 2019*, Lagos, Nigeria, 2019: Society of Petroleum Engineers, https://doi.org/10.2118/198796-MS

[3] E. Teymori, M. Abdideh, and M. A. Gholamzadeh, "The zoning and characterisation of heterogeneous carbonate reservoirs based on the concept of flow units," *Applied Earth Science: Transactions of the Institute of Mining and Metallurgy*, Article pp. 122-132, 2020, https://doi.org/10.1080/25726838.2020.1791678

[4] H. H. Mahmood and O. F. Al-Fatlawi, "Construction of comprehensive geological model for an Iraqi Oil Reservoir," *The Iraqi Geological Journal*, vol. 54, no. 2F, pp. 22-35, 2021, https://doi.org/10.46717/igj.54.2F.3ms-2021-12-20

[5] A. M. Al-Heeti, O. F. Al-Fatlawi, and M. M. Hossain, "Evaluation of the Mishrif Formation Using an Advanced Method of Interpretation," *Iraqi Journal of Chemical and Petroleum Engineering*, vol. 24, no. 2, pp. 41-51, 2023, https://doi.org/10.31699/IJCPE.2023.2.5

[6] S. A. Jassam, A.-F. Omer, and C. H. Canbaz, "Petrophysical Analysis Based on Well Logging Data for Tight Carbonate Reservoir: The SADI Formation Case in Halfaya Oil Field," *Iraqi Journal of Chemical and Petroleum Engineering*, vol. 24, no. 3, pp. 55-68, 2023, https://doi.org/10.31699/IJCPE.2023.3.6

[7] M. Kennedy, "Petrophysical Properties," in *Developments in Petroleum Science*, vol. 62, 2015, pp. 21-72, https://doi.org/10.1016/B978-0-444-63270-8.00002-5

[8] O. Al-Fatlawi, M. Hossain, N. Patel, and A. Kabir, "Evaluation of the potentials for adapting the multistage hydraulic fracturing technology in tight carbonate reservoir," in *SPE Middle East Oil and Gas Show and Conference*, Manama, Bahrain, 2019: SPE, p. D022S054R002, https://doi.org/10.2118/194733-MS

[9] S. A. Jassam and O. Al-Fatlawi, "Development of 3D Geological Model and Analysis of the Uncertainty in a Tight Oil Reservoir in the Halfaya Oil Field," *The Iraqi Geological Journal*, vol. 56, no. 1B, pp. 128-142, 2023, https://doi.org/10.46717/igj.56.1B.10ms-2023-2-18

[10] R. O. Baker, H. Yarranton, and J. Jensen, *Practical reservoir engineering and characterization* (Practical Reservoir Engineering and Characterization). Gulf Professional Publishing, 2015, pp. 1-534.

[11] Z. Rui *et al.*, "A quantitative oil and gas reservoir evaluation system for development," *Journal of Natural Gas Science and Engineering*, Article vol. 42, pp. 31-39, 2017, https://doi.org/10.1016/j.jngse.2017.02.026

[12] O. F. Al-Fatlawi, "Numerical simulation for the reserve estimation and production optimization from tight gas reservoirs," Curtin University, 2018.

[13] O. Salman, O. Al-Fatlawi, and S. Al-Jawad, "Reservoir Characterization and Rock Typing of Carbonate Reservoir in the Southeast of Iraq," *The Iraqi Geological Journal*, vol. 56, no. 1A, pp. 221-237, 2023, https://doi.org/10.46717/igj.56.1A.17ms-2023-1-29

[14] P. Bertier, T. Seemann, B. Krooss, and H. Stanjek, "Water vapour sorption by shales," in *5th EAGE Shale Workshop: Quantifying Risks and Potential*, Catania, Italy, 2016, pp. 27-31, https://doi.org/10.3997/2214-4609.201600394

[15] K. M. Sundaram, "Pores and pore space," in *Developments in Petroleum Science*, vol. 76: Elsevier, 2022, pp. 1-29, https://doi.org/10.1016/B978-0-444-64169-4.00007-9

[16] I. Woo, "Pore Size Redistribution by Laboratory Weathering Tests on Sedimentary rocks," Copernicus Meetings, 2023, https://doi.org/10.5194/egusphere-egu23-1518

[17] A. K. Farouk and A. A. Al-haleem, "Integrating Petrophysical and Geomechanical Rock Properties for Determination of Fracability of an Iraqi Tight Oil Reservoir," *The Iraqi Geological Journal*, vol. 55, no. 1F, pp. 81-94, 2022, https://doi.org/10.46717/igj.55.1F.7Ms-2022-06-22

[18] R. Khisamov *et al.*, "Well logging data interpretation in oil and gas source rock sections based on complex petrophysical and geochemical analysis results," in *SPE Russian Petroleum Technology Conference*, 2018: OnePetro, https://doi.org/10.2118/191675-18RPTC-MS

[19] K. N. Ibekwe *et al.*, "Complete overview of reservoir characterisation in sedimentary basins," *Journal of Energy Research and Reviews*, vol. 1, 2023, https://doi.org/10.22541/essoar.167689978.89415074/v1

[20] M. T. Galli, M. Arcangeli, and N. Ceresa, "Quantitative evaluation of the uncertainty associated to the most critical petrophysical parameters: An application in thin beds," in *Offshore Mediterranean Conference and Exhibition 2019, OMC 2019*, Ravenna, Italy, 2019.

[21] Z. A. Al-Rubiay and O. F. Al-Fatlawi, "A Survey of Infill Well Location Optimization Techniques," *The Iraqi Geological Journal*, vol. 56, no. 1E, pp. 43-51, 2023, https://doi.org/10.46717/igj.56.1E.4ms-2023-5-14

[22] E. A. Agbauduta, "Evaluation of in-fill well placement and optimization using experimental design and genetic algorithm," MASTER OF SCIENCE, Department of Petroleum Engineering, The African University of Science and Technology, 2014.

[23] M. Alfarraj and G. AlRegib, "Petrophysical property estimation from seismic data using recurrent neural networks," presented at the SEG Technical Program Expanded Abstracts 2018, Anaheim, California, 2018, https://doi.org/10.1190/segam2018-2995752.1

[24] J. Kristensson, "Formation evaluation of the Jurassic Stø and Nordmela formations in exploration well 7220/8-1, Barents Sea, Norway," Master, Department of Geology, Lund University, Sölvegatan, 2016.

[25] A. M. Al-Heeti and O. F. Al-Fatlawi, "Review of Historical Studies for Water Saturation Determination Techniques," *The Iraqi Geological Journal*, vol. 55, no. 2A, pp. 42-62, 2022, https://doi.org/10.46717/igj.55.2A.4Ms-2022-07-20

[26] D. Tiab and E. C. Donaldson, *Petrophysics: theory and practice of measuring reservoir rock and fluid transport properties*. Gulf professional publishing, 2015.

[27] K. Ezebialu, M. Ubituogwale, E. Odegua, and A. Idehen, "Field development planning based on static, dynamic and geomechanical modelling of X field, Niger delta, Nigeria," in *Society of Petroleum Engineers - SPE Nigeria Annual International Conference and Exhibition 2020, NAIC 2020*, 2020: Society of Petroleum Engineers, https://doi.org/10.2118/203730-MS

[28] J. Lai *et al.*, "Geophysical well-log evaluation in the era of unconventional hydrocarbon resources: a review on current status and prospects," *Surveys in Geophysics*, vol. 43, no. 3, pp. 913-957, 2022, https://doi.org/10.1007/s10712-022-09705-4

[29] A. K. A. Mohammed, J. K. Radhi, and S. Z. Ali, "Well logs data prediction of the Nahr Umr and Mishrif formations in the Well Noor-10, Southern Iraq," *The Iraqi Geological Journal*, vol. 53, no. 2A, pp. 50-67, 2020, https://doi.org/10.46717/igj.53.2A.4Rw-2020-08-04

[30] S. S. Abdulrahman, M. S. Alkubaisi, and G. H. Al-Shara'a, "Formation evaluation for Jeribe Formation in the Jaria Pika gas field," *The Iraqi Geological Journal*, vol. 53, no. 2F, pp. 83-93, 2020, https://doi.org/10.46717/igj.53.2F.6Ms-2020-12-29

[31] M. H. Mahmood and D. J. Sadeq, "Study of petrophysical properties of a Yamama reservoir in Southern Iraqi oil field," in *AIP Conference Proceedings*, 2023, vol. 2839, no. 1: AIP Publishing, https://doi.org/10.1063/5.0167933

[32] M. Mazeel, "Siba gas field development plan: Subsurface Uncertainties and Economic Criteria," *Middle East Economic Survey*, vol. 53, no. 27, 2010.
[33] H. Y. Ali, G. M. Farman, and M. H. Hafiz, "Study of Petrophysical Properties of the Yamama Formation in Siba Oilfield," *The Iraqi Geological Journal*, vol. 54, no. 2C, pp. 39-47, 2021, https://doi.org/10.46717/igj.54.2C.4Ms-2021-09-23
[34] M. M. Al-Ghuribawi and R. F. Faisal, "An Integrated Microfacies and Well Logs-Based Reservoir Characterization of Yamama Formation, Southern Iraq," *Iraqi Journal of Science*, vol. 62, no. 10, pp. 3570-3586, 2021, https://doi.org/10.24996/ijs.2021.62.10.16
[35] F. Al-Musawi, A. M. Abed, and R. M. Idan, "Acquisition and Preparation of 3D Seismic Data for Pre-Stack Inversion at Siba Oilfield, Southeastern Iraq," *Iraqi Journal of Science*, vol. 63, no. 8, pp. 3555-3569, 2022, https://doi.org/10.24996/ijs.2022.63.8.28
[36] A. M. Handhal, M. Q. Aljazaeri, W. Abdulnaby, F. R. Ettensohn, A. M. Al-Abadi, and M. J. Ismail, "Relationship between structural style and the petroleum system in the siba gas field, southern Iraq," *Marine and Petroleum Geology*, vol. 155, p. 106396, 2023/09/01/ 2023, https://doi.org/10.1016/j.marpetgeo.2023.106396
[37] A. H. Fayadh and M. H. E. Nasser, "Well Log Analysis and Interpretation for Khasib, Tanuma, and Sa'di formations for Halfaya Oil Field in Missan Govenorate-Southern Iraq," *Iraqi Journal of Science*, vol. 59, no. 1C, 2018.
[38] R. A. M. Hussien and M. Ahmed, "Petrophysical Evaluation of Shaly Sand Reservoirs in Palouge-Fal Oilfield, Melut Basin, South East of Sudan," *Journal of Science and Technology*, vol. 13, no. 2, 2012.
[39] A. Al-Hasani, I. M. Saaed, A. M. Salim, and H. T. Janjuhah, "Advanced Porosity Modeling and Lithology Analysis Based on Sonic Log and Core Data for Arkose Sandstone Reservoir: Habban Field," in *ICIPEG 2016*, Singapore, M. Awang, B. M. Negash, N. A. Md Akhir, L. A. Lubis, and A. G. Md. Rafek, Eds., 2017 2017: Springer Singapore, pp. 617-641, https://doi.org/10.1007/978-981-10-3650-7_54
[40] P. Spooner, "Lifting the fog of confusion surrounding clay and shale in petrophysics," in *SPWLA Annual Logging Symposium*, 2014: SPWLA, pp. SPWLA-2014-VV.
[41] P. S. Adisoemarta, G. A. Anderson, S. M. Frailey, and G. B. Asquith, "Saturation Exponent n in Well Log Interpretation: Another Look at the Permissible Range," in *SPE Permian Basin Oil and Gas Recovery Conference*, 2001, vol. All Days, SPE-70043-MS, https://doi.org/10.2118/70043-MS
[42] M. M. Al-Hilali, M. J. Zein Al-Abideen, F. Adegbola, W. Li, and A. M. Avedisian, "A Petrophysical Technique to Estimate Archie Saturation Exponent (n); Case Studies in Carbonate and Shaly-Sand Reservoirs – IRAQI Oil Fields," in *SPE Annual Caspian Technical Conference & Exhibition*, Baku, Azerbaijan, 2015, vol. All Days, SPE-177331-MS, https://doi.org/10.2118/177331-MS
[43] Z. Bassiouni, *Theory, measurement, and interpretation of well logs*. Society of Petroleum Engineers. 1994.
[44] H. S. Salem and G. V. Chilingarian, "The cementation factor of Archie's equation for shaly sandstone reservoirs," *Journal of Petroleum Science and Engineering*, vol. 23, no. 2, pp. 83-93, 1999/08/01/ 1999, https://doi.org/10.1016/S0920-4105(99)00009-1
[45] Y. X. Z. C. T. C. W. M. Cheng Dawei, "Logging-lithology identification methods and their application: A case study on Chang 7 Member in central-western Ordos Basin, NW China," *China Petroleum Exploration*, vol. 21, no. 5, pp. 117-126, 2016.
[46] P. W. Glover, "A new theoretical interpretation of Archie's saturation exponent," *Solid Earth*, vol. 8, no. 4, pp. 805-816, 2017, https://doi.org/10.5194/se-8-805-2017

الخواص البتروفيزيائية لتكوين اليمامة (YC) في حقل سيبة

زينب عبد الكريم هادي [١]، عمر فالح الفتلاوي [١، ٢]، علي كدخد [٣، *]

١ قسم هندسة النفط، كلية الهندسة، جامعة بغداد، العراق
٢ مدرسة غرب استراليا للمناجم: المعادن، الطاقة والهندسة الكيمياوية، جامعة كيرتن، استراليا
٣ قسم علوم الأرض، كلية العلوم الطبيعية، جامعة تبريز، إيران

الخلاصة

في جنوب العراق، كان تكوين اليمامة مصدرًا رئيسيًا للكربونات منذ العصر الطباشيري السفلي. تغطي هذه الدراسة حقل سيبا الواقع جنوب شرق العراق. سيتم تخصيص هذه الورقة لوحدة دراسة YC. الخطوة الأكثر أهمية في إدارة المكامن هي التوصيف الفيزيائي الصخري. الهدف الأساسي من هذا البحث هو تقييم خصائص الخزان والصخور لتكوين اليمامة (YC) في منطقة سيبا. تتضمن السجلات الممتازة التي يمكن الوصول إليها قراءات الصوت، والكثافة، والنيوترون، وأشعة غاما، و SP، والمقاومة. قام برنامج الفيزياء البتروفيزيائية التفاعلية (IP4.4) بفحص وتقدير الخصائص البتروفيزيائية مثل حجم الطين والمسامية والتشبع بالماء، وكان الأسلوب الأمثل هو حساب كثافة النيوترونات وحجم الطين باستخدام طريقة أشعة جاما (VclGR) ، حيث كانت 0.264 في SB −6 لأنها لا تتأثر بأي شيء. تم اختيار طريقة أرشي بسبب ملاءمتها للحجر الجيري. تم تحديد علم الصخور وعلم المعادن في التكوينات باستخدام قطع M−N المتقاطعة؛ أظهر الرسم البياني أن التكوين كان مكونًا من الحجر الجيري. تم تحديد معامل Archie باستخدام مخطط الالتقاط ومقاومة الماء للتكوين من مؤامرة الالتقاط وسجل SP حيث كانت النتائج متشابهة في جميع الآبار(R_W = 0.016، m = 2.08 ، n = 2.3، a = 1.1) بالإضافة إلى ذلك، يتمتع القسم الأعلى من التكوين بصفات مكمن جيدة مثل الكثافة (2.368g/cc) والمسامية كانت (PHIE = 0.117) فيSB−6 .

الكلمات الدالة: الخواص البتروفيزياوية, تكوين اليمامة , تمثيل المكمن, حقل السيبة.